Proceedings of the Thirty-sixth (2026) International Ocean and Polar Engineering Conference **www.isope.org**
Orlando, Florida, USA, May 31-June 5, 2026

ISBN 978-1-880653-72-2; ISSN 1098-6189

Comparison Study of Finite-volume and Spectral Element Method on Wall Pressure Fluctuations in Turbulent Channel Flow

Gaoyang Shen, Wenbin Zhang, Weiwen Zhao, Decheng Wan[*]

Computational Marine Hydrodynamic Lab (CMHL), School of Ocean and Civil Engineering,
Shanghai Jiao Tong University, Shanghai, China
[*]Corresponding author

ABSTRACT

Accurate estimation of spatial and temporal correlations is crucial to predicting the power spectral density (PSD) of wall pressure fluctuation in wall-bounded turbulence, especially the high-frequency components. This study investigates turbulent channel flow at Re_τ=1000by comparing simulations from two open-source codes: the second-order finite-volume code OpenFOAM and the high-order spectral element code Neko. The objective of this study is to evaluate the effects of grid resolution and discretization scheme on spatial and temporal correlation characteristics of the wall pressure fluctuation. The temporal correlation functions are constructed based on the fluctuating pressure obtained from the simulation results. On this basis, features such as coherence length are extracted from the temporal correlation functions. The results reveal that an excessively coarse grid resolution with second-order discretization schemes overpredicts the temporal correlation of the wall pressure fluctuations, which results in the underestimation of high-frequency components in the PSD of the wall pressure fluctuation. In contrast, the high-order schemes improve the predictive accuracy of wall pressure fluctuations with under-resolved grid resolution and are closer to the calculation results of fine grids in the high-frequency range.

KEY WORDS: temporal correlations, large eddy simulation, wall pressure fluctuation, turbulent channel flow

INTRODUCTION

Wall pressure fluctuations originate from the motion of coherent turbulent structures within the turbulent boundary layer. Their power spectral density (PSD) reflects the energy distribution and spatiotemporal evolution of turbulent structures across different scales. For theoretical research into turbulence mechanisms, the generation, evolution, and breakdown of coherent structures in the turbulent boundary layer produce distinct pressure fluctuations at the wall. Large-scale vortex convection generates low-frequency, high-energy fluctuations, while the breakdown of small-scale eddies dominates the high-frequency range. The PSD curve can be used to verify and refine theoretical models of turbulence, thereby deepening the understanding of turbulence energy cascade, production, and dissipation mechanisms at full scale.

From the engineering perspective, predicting the power spectrum of wall pressure fluctuations can be directly translated into load inputs and noise sources. It can provide input for models subjected to strong turbulence-induced random pressure loads, such as the aerodynamic kit of high-speed aircraft, fuel pipelines of launch vehicles, and heat exchanger tube bundles in nuclear power plants, ensuring the safety of such structures under intense turbulent flow. In the case of high-speed vehicles, surfaces subjected to fluctuating pressure for a long time would face the risk of structural fatigue (Bull, 1996). For certain stealth underwater vehicles, flow noise generated by turbulent wall pressure fluctuations is a primary noise source (Shubham *et al*., 2023). PSD analysis can further quantify its intensity and frequency distribution, providing guidance for equipment design.

The credibility of using numerical simulations to solve for the wall pressure spectrum is highly dependent on spatial discretization errors, related to the number of degrees of freedom. Insufficient grid density can modify the sweeping and convection processes of near-wall coherent structures through numerical dissipation and dispersion, further influencing the decorrelation rate and spectral bandwidth of wall pressure. Therefore, a systematic evaluation of the effects of grid density is crucial.

He *et al.* (2017) systematically reviewed the classical framework for spatio-temporal correlation studies in turbulence, discussing models such as Taylor's frozen turbulence hypothesis, random sweeping, and local stretching from Eulerian and Lagrangian perspectives to explain temporal decorrelation processes. They pointed out that spatiotemporal correlations are a key statistical foundation for developing time-accurate turbulence models and turbulence-induced noise modeling (He *et al*., 2017). Building on this, Wu and He further summarized the definition, measurement, and reconstruction methods of spatiotemporal energy spectra from the (k, ω) wavenumber-frequency domain, emphasizing that real shear turbulence has a finite spectral bandwidth and that the convection ridge line and spectral broadening jointly determine the scale-dependent characteristics of propagation velocity and time scales (Wu and He, 2021).

Regarding the predictive capability of LES for spatiotemporal correlations, Guo *et al.*(2012) compared DNS and LES results for spatiotemporal correlations in channel flow. They found that LES using eddy-viscosity-type subgrid-scale (SGS) models often overpredicts correlations, attributing this to the absence of stochastic backscatter effects in the eddy-viscosity closure, resulting in a smoother resolved field and slower decorrelation. This work also used an elliptical model parameterized by propagation and sweeping velocities to provide a unified framework for analyzing correlation differences under various models and numerical settings (Guo *et al*., 2012).

In the study of near-wall structures using Wall-Modeled LES (WMLES), Fan *et al.*(2025) utilized (k_x,,ω) spectra to reveal the convection ridge characteristics between wall pressure and coherent structures, identifying the buffer layer as the primary source region for wall pressure fluctuations. The study also highlighted systematic biases of WMLES in predicting low-wavenumber wall pressure fluctuations and emphasized that insufficient wall-normal resolution in the buffer layer significantly affects the prediction of near-wall fluctuations and wall pressure spectra (Fan *et al.*, 2025).

The Spectral Element Method (SEM), introduced by Patera, combines the geometric flexibility of the Finite Element Method with the high-order accuracy of spectral methods, providing a high-precision discretization for the incompressible Navier-Stokes equations (Patera, 1984). Karniadakis further discussed the implementation of SEM in complex geometries and its application in laminar and turbulent flows (Karniadakis, 1989). For Spectral Element LES, Blackburn and Schmidt proposed filtering and dynamic estimation strategies tailored for SEM discretization, providing methodological references for implementing wall-bounded turbulence LES (Blackburn and Schmidt, 2003). At the high-performance implementation level, Jansson *et al*. proposed the Neko framework, targeting high-fidelity CFD computations with an emphasis on portability and scalability (Jansson *et al.*, 2024). Concurrently, Karp *et al.*(2022) discussed communication overhead reduction and implementation on new hardware platforms for key linear solvers in high-order finite element and spectral element methods, providing support for efficient solution of Poisson subproblems (Karp *et al*., 2022b, 2022a).

In summary, the spectral element method solver, Neko, demonstrates high efficiency and performance in computing wall fluctuations. However, under large eddy simulation (LES) conditions, the advantages of its computational results over those obtained from the finite volume method remain unclear and require explicit quantitative analysis.

This study aims to compare the effects of grid resolution on the calculation of pressure fluctuation power spectra between the finite volume method solver OpenFOAM and the high-order spectral element method solver Neko. To this end, we varied the grid density to obtain wall pressure time series signals. The autocorrelation function $R_P(\tau)$ was computed from these signals to quantify temporal and spatial correlation. The Welch method was employed to construct the temporal wall pressure power spectrum, enabling a joint evaluation of numerical convergence and error characteristics in both the time and frequency domains.

METHODS

OpenFOAM

OpenFOAM employs an LES model for turbulence simulation:

$$\frac{\partial \bar{u}_i}{\partial x_i} = 0 \tag{1}$$

$$\frac{\partial \bar{u}_i}{\partial t} + \frac{\partial (\bar{u}_i \bar{u}_j)}{\partial x_j} = -\frac{1}{\rho}\frac{\partial \bar{p}}{\partial x_i} + \nu \frac{\partial^2 \bar{u}_i}{\partial x_j \partial x_j} - \frac{\partial \tau_{ij}}{\partial x_j} \tag{2}$$

Where τ_{ij} is the subgrid-scale (SGS) stress tensor, which is modeled as:

$$\tau_{ij} - \frac{1}{3}\tau_{kk}\delta_{ij} = -2\nu_t \bar{S}_{ij} \tag{3}$$

where $\bar{S}_{ij} = \frac{1}{2}\left(\frac{\partial \bar{u}_i}{\partial x_j} + \frac{\partial \bar{u}_j}{\partial x_i}\right)$ is the resolved strain-rate tensor, and ν_t is the subgrid eddy viscosity provided by the Wall-Adapting Local Eddy-visc osity (WALE) model:

$$\nu_t = (C_w \Delta)^2 \frac{\left(S_{ij}^d S_{ij}^d\right)^{3/2}}{\left(\bar{S}_{ij}\bar{S}_{ij}\right)^{5/2} + \left(S_{ij}^d S_{ij}^d\right)^{5/4}} \tag{4}$$

with

$$S_{ij}^d = \frac{1}{2}\left(\bar{g}_{ij}^2 + \bar{g}_{ji}^2\right) - \frac{1}{3}\delta_{ij}\bar{g}_{kk}^2 \tag{5}$$

in which C_W=0.325 is the WALE model constant, and $\Delta=(\Delta_x\Delta_y\Delta_z)^{1/3}$ is the filter width based on the local grid spacing.

Neko

The Neko solver employs the spectral element method to solve the Navier-Stokes equations, with the turbulence modeling approach consistent with OpenFOAM using LES, and the WALE model as the subgrid-scale model, where the parameters are kept consistent with the OpenFOAM case.

Spatial discretization employs the spectral element method with a polynomial order of N=5 on hexahedral elements. An equal-order PN−PN formulation is used for velocity and pressure, stabilized through dealiasing and implicit numerical dissipation. Time integration uses a third-order scheme. Linear systems arising from the implicit treatment are solved iteratively, using the pressure Poisson equation with GMRES preconditioned by geometric multigrid, and the velocity Helmholtz equation with conjugate gradient and Jacobi preconditioning.

Model Setup

The research object is turbulent channel flow. The finite volume method solver OpenFOAM and the high-order spectral element method solver Neko were used for the simulations.

For the OpenFOAM solver, the friction Reynolds number Re_τ was set to 1000, with a channel half-height of 1 m. The computational domain had a streamwise length of 2π and a spanwise length of π. Two different meshes (coarse and fine) with different grid density in the streamwise and spanwise direction were adopted.

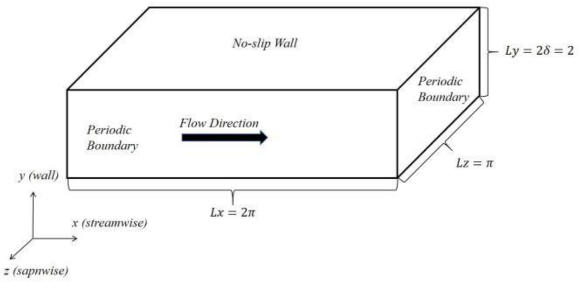

Fig. 1 Schematic of Model Setup

For the Neko solver, as shown in Fig. 1, the computational domain had a streamwise length of 2π and a spanwise length of π. The friction Reynolds number was maintained at Re_τ=1000, with a channel half-height of 1 m. During element partitioning, three meshes were selected with element distributions of 55×24×30, 55×20×30 and 40×24×25 respectively, all using a polynomial order of 5. The corresponding degrees of freedom were approximately 5.04M, 4.2M, and 3.06M. The calculation tolerance for velocity and pressure was 1e-6. For OpenFOAM cases, the output frequency was 100 Hz, the total simulation time was 200 seconds, and the last 100 seconds were used as target data to compute the pressure power spectral density. For Neko cases, the output frequency was 100Hz, the total simulation time was 200 seconds, and the last 100 seconds were used as target data. The simulation cases are summarized in Table 1.

Table 1 Summary of Simulation Cases

Cases	Solver	Nx*Ny*Nz	Freq
OpenFOAM	OpenFOAM	314*216*314	100
Neko1	Neko	55*24*30(n=5)	100
Neko2	Neko	55*20*30(n=5)	100
Neko3	Neko	40*24*25(n=5)	100

Boundary Conditions

Periodic boundary conditions were applied in the streamwise and spanwise directions:

$$u\left(x+L_x,y,z,t\right)=u(x,y,z,t) \quad (6)$$

$$u(x,y,z+L_z,t)=u(x,y,z,t) \quad (7)$$

No-slip conditions were applied at the walls:

$$u\left(y=\pm h,t\right)=0 \quad (8)$$

Model Validation

The time-averaged boundary layer velocity profile from 50-100 seconds was used for validation. 5000 equally spaced points were taken along the channel half-height, and their velocities were output. The dimensionless velocity $u_+=u/u_\tau$ and wall distance $y_+=yu_\tau/v$ were calculated to plot the u_+/y_+ curve. This curve was compared against the u_+/y_+ curve obtained from the Johns Hopkins Turbulence Database for the same Re_τ=1000, as shown in Fig. 2. The dimensionless velocity profile u_+ as a function of y_+ is in good agreement with the Spalding law of the wall. The comparison revealed a high degree of similarity between the results computed using OpenFOAM and Neko and those from the database and empirical formula. However, given that the validation is based on the mean velocity profile, this result merely provides preliminary validation of the correctness of the computational case used in this study.

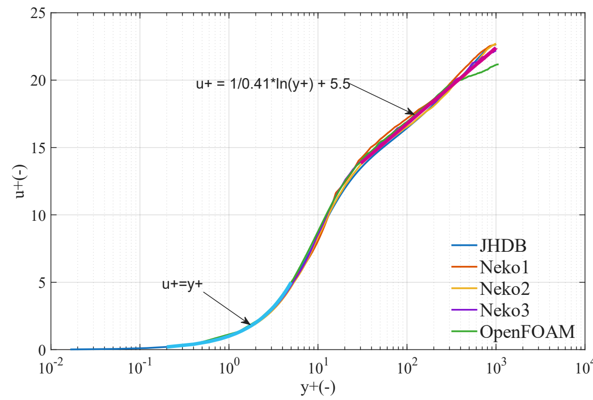

Fig. 2 Mean Streamwise Velocity Profile

RESULTS AND DISCUSSION

In this section, we first computed the wall pressure variation $p(t)$ over time for Re_τ=1000 in both solvers. The autocorrelation function $R_P(\tau)$ was then calculated using Equation:

$$R_p\left(\tau\right)=\int_0^{T-t} p\left(t\right)p\left(t+\tau\right)dt,\left(\tau>0\right) \quad (9)$$

Considering robustness and interference from numerical noise, the Welch method was employed to obtain the wall pressure power spectrum. Data were divided into segments of 500 points each, using a Hanning window with 50% overlap.

Autocorrelation Function Analysis

Fig. 3 shows the time autocorrelation functions for four cases. Comparing the three cases computed using the spectral element solver Neko, it can be observed that during the decay of signal correlation, the coherence lengths are very similar and converge to a specific value, indicating that the numerical accuracy has reached a relatively high level. Furthermore, as the time lag increases, the correlation with the original signal remains weak, which is attributed to the rapid emergence and dissipation of a large number of small-scale vortex structures in turbulent flows, leading to a sharp decrease in correlation. Meanwhile, the influence of large-scale vortex structures is comparatively weak, causing the autocorrelation to drop significantly after a time lag exceeding one second. The comparison among these three cases also suggests that grid resolution does not have a significant impact on the time autocorrelation function from SEM results.

Comparing the autocorrelation functions obtained from the finite volume method and the spectral element method, it is evident that the finite volume method yields a considerably longer coherence length than the spectral element method. Even after a time lag of more than one second, the signal still retains some correlation with the original signal, and this correlation persists over longer time lags. This behavior is due to the fact that large eddy simulation filters out small-scale coherent structures, and compared to LES with the spectral element method, LES with the finite volume method exhibits higher numerical dissipation. This is inherent to the low-order discretization schemes used in the finite volume method. Under such high numerical dissipation, small-scale vortex structures tend to be dissipated more effectively in the LES framework. Given that both methods use a sampling rate of 100 Hz, small-scale vortex structures are more difficult to capture with the finite volume method, whereas the spectral element method can effectively resolve them. This also indirectly indicates that, under the current grid resolution, the resolution of the finite volume method remains insufficient, and further grid refinement may contribute to improving the accuracy of the results.

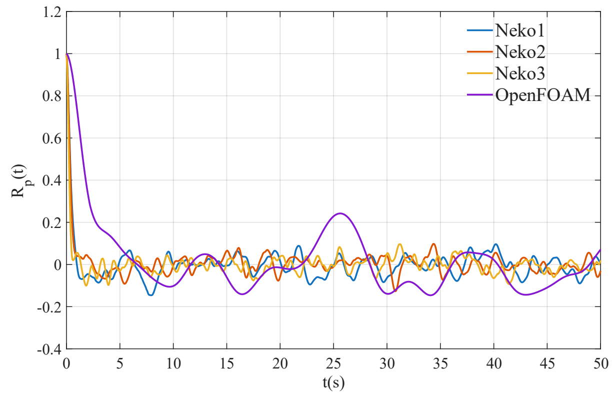

Fig. 3 Autocorrelation Function from LES

PSD Analysis

Fig. 4 presents the power spectral density (PSD) curves of pressure time histories obtained from the four computational cases. Both axes are normalized using the friction velocity and viscosity. It can be observed that the curves generally conform to the Goody wall-pressure spectral model, exhibiting a weak positive slope in the low-frequency range, reaching a peak in the mid-frequency range, and displaying a rapid decline at high frequencies. For comparison, we include the direct numerical simulation (DNS) results of B. Yang *et al*. (Note: their time-domain PSD curves were obtained by integrating the wavenumber–frequency spectra, resulting in smoother curves compared to the present study).

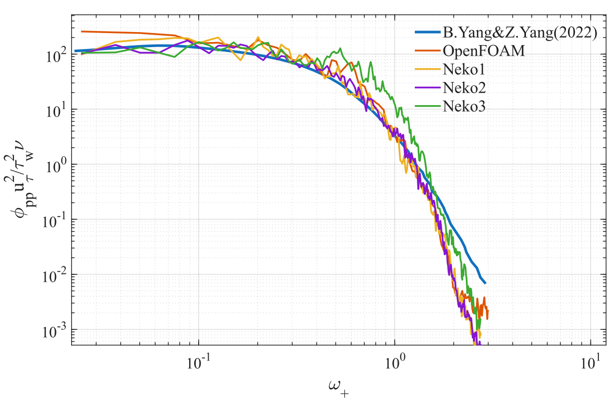

Fig. 4 Temporal PSD

For the four cases in the present study, regardless of whether the spectral element method or the finite volume method is employed, the PSD curves are consistently lower than the reference in the low-frequency range ($\omega+ < 0.5$). Except for Neko3, the other three cases begin to deviate toward lower values from $\omega+ = 1$ onward. This behavior is characteristic of insufficient spatial resolution: turbulent energy follows the physical mechanism of the energy cascade, wherein energy is transferred from large-scale vortex structures to progressively smaller scales and ultimately dissipated. When the grid resolution is inadequate, the energy cascade is effectively disrupted. As smaller-scale vortex structures cannot be resolved, the energy cannot be further transferred and is instead dissipated via numerical dissipation inherent to the numerical method. Consequently, energy is dissipated prematurely before reaching the high-frequency range. This results in an over-prediction of the PSD in the low-frequency range relative to the DNS reference, while the PSD becomes under-predicted as frequency increases. The underlying cause is that numerical dissipation replaces the physical dissipation that would otherwise occur in a real turbulent flow.

Comparing Cases Neko1 and Neko2 reveals that the time-domain PSD is not highly sensitive to the wall-normal grid resolution, provided that the near-wall resolution satisfies $y+ <1$. In contrast, Case Neko3 exhibits a notable anomaly: the over-prediction of the PSD occurs at a lower frequency and is more pronounced. Compared with Neko1, the only difference lies in the streamwise and spanwise grid densities, suggesting that the resolution in these two directions critically influences the accuracy of the PSD.

A comparison between the finite volume method and the spectral element method shows that the accuracy of OpenFOAM is slightly lower than that of Neko2. In the low-frequency range, the finite volume method exhibits a more severe over-prediction of the PSD, and the numerical contamination appears at an earlier frequency. This indicates that further refinement of the grid resolution in the finite volume method could still contribute to improved accuracy, reinforcing our earlier argument regarding its insufficient grid resolution.

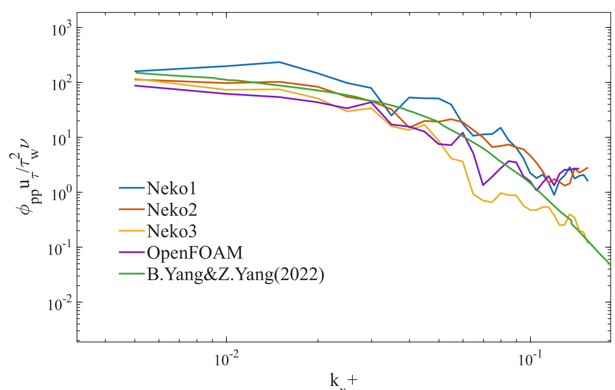

Fig. 5 Spatial PSD (Streamwise)

Fig. 5 presents a comparison of the spatial power spectral densities in spanwise, obtained from finite-volume method and the high-order spectral element method (SEM). For streamwise direction, the sampling length was set to 2π m with 314 measurement points. The wavenumber and power spectral density were non-dimensionalized using $k_x^+ = k_x \nu / u_\tau$.

Fig. 6 presents a comparison of the spatial power spectral densities in spanwise, obtained from finite-volume method and the high-order spectral element method (SEM). For spanwise direction, the sampling length was set to π m with 314 measurement points. The nondimensionalization procedure is the same as that used for the streamwise power spectral density.

From Fig. 5 and Fig. 6, it can be observed that Cases Neko1 and Neko2 yield results that are closer to the DNS reference than those obtained from the OpenFOAM case. In contrast to the time-domain power spectral density (PSD) results, the four cases do not exhibit clear convergence, and all show a certain degree of deviation from the DNS data. This is primarily attributed to insufficient sampling resolution. Unlike the time-domain PSD, which is constrained by the computational time step, the sampling resolution of the spatial power spectral density is limited by the grid spacing. When the sampling interval falls below the grid resolution, interpolation inevitably introduces discrepancies from the true solution, preventing the capture of features beyond the current grid resolution.

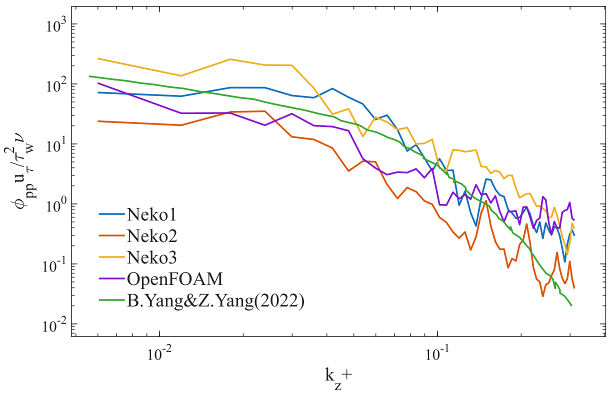

Fig. 6 Spatial PSD (Spanwise)

This effect is particularly pronounced for the spectral element method. As discussed previously, in the correlation analysis of temporal pressure fluctuations, Case Neko1 demonstrates higher accuracy than the OpenFOAM case. However, when considering spatial pressure fluctuations, the spectral element method exhibits a notable increase in error. This is because the spectral element method employs a coarser grid and relies on non-uniform node distributions to mitigate the Runge phenomenon. Consequently, its capability to resolve certain small-scale vortex structures in space is compromised, and the resulting spatial power spectral density does not show a significant improvement in accuracy compared to OpenFOAM.

Energy Integral Analysis

To further quantify the influence of temporal correlation on the energy within specific frequency bands, we adopted the high-fidelity DNS results of Yang and Yang (2022) as a reference and introduced the energy integral :

$$E_f = \int_{f1}^{f2} S_{pp}(f) df \tag{10}$$

$$\eta_i = \frac{E_{fi} - E_{DNS}}{E_{DNS}} \times 100\% \tag{11}$$

where $S_{pp}(f)$ denotes the power spectral density of wall pressure fluctuations, ΔE represents the total energy in the range of one-third octave band given by ISO, and η_i represents the energy integral deviation rate. The resulting energy deviations are presented in Fig. 7.

From the cumulative energy deviation curves of the time-domain power spectral density, it can be observed that all four cases overestimate the integrated energy in the low-frequency range. Cases Neko1 and Neko2 exhibit relatively small relative deviations in cumulative energy compared to the DNS results. The OpenFOAM case shows a pronounced energy deviation in the mid-frequency range. In contrast, Case Neko3, owing to its coarser streamwise and spanwise resolution, displays an overestimation of the cumulative energy across a broad range of frequencies, with a clear underestimation only emerging for frequencies exceeding 12 Hz. The remaining three cases generally exhibit an increasing energy deviation with frequency in the high-frequency range. These observations further support the findings discussed above: the capture of high-frequency signals is highly dependent on the improvement of grid resolution, and insufficient resolution leads to an overestimation of low-frequency power and an underestimation of high-frequency power.

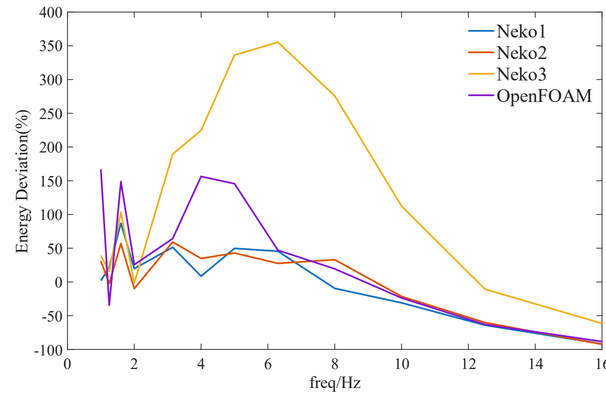

Fig. 7 Energy Deviation (One-third Octave Band)

CONCLUSION

In this study, we compare the results of the finite volume method and the spectral element method, both employing large eddy simulation with the WALE subgrid model, in the spatial and temporal correlation analysis of wall pressure fluctuations, and examine the influence of grid resolution on the results.

The findings reveal that insufficient grid resolution leads to an overestimation of the power spectral density in the low-frequency range and an underestimation in the high-frequency range. This behavior arises because inadequate grid resolution disrupts the turbulent energy cascade, causing numerical dissipation inherent to the numerical method to replace the physical dissipation of turbulence. As a result, dissipation occurs prematurely, leading to elevated low-frequency power and reduced high-frequency power.

In the analysis of spatial correlation, the spectral element method, owing to its coarser grid and non-uniform nodal distribution under the configurations considered in this study, does not exhibit a significant difference from the finite volume method. This suggests that spatial correlation imposes stringent requirements on the streamwise and spanwise grid resolutions, whereas the wall-normal resolution is less critical, provided that the near-wall resolution satisfies $y+ < 1$.

The spectral element method demonstrates superior performance to the finite volume method in temporal correlation, attributable to the lower numerical dissipation associated with its high-order formulation. Moreover, for an equivalent level of accuracy, the total number of degrees of freedom required by the spectral element method is approximately one-fifth of that required by the finite volume method.

Due to the limited number of cases and the total data samples available in this study, this study only ensures a certain degree of similarity in mesh partitioning between the SEM and FVM methods in three directions. Further investigation into grid refinement strategies and the achievable accuracy limits for a given number of degrees of freedom could not be conducted.

Additionally, the computational time step represents another important factor. Future work may focus on optimizing grid refinement strategies while simultaneously selecting appropriate time steps, aiming to enhance the accuracy of wall pressure predictions while maintaining a favorable cost–accuracy balance relative to direct numerical simulation. Such efforts would provide clearer technical guidance for engineering applications that require a trade-off between computational efficiency and predictive fidelity.

ACKNOWLEDGEMENTS

This work was supported by the National Natural Science Foundation of China (52131102), to which the authors are most grateful.

REFERENCES

Blackburn, HM, and Schmidt, S (2003). "Spectral Element Filtering Techniques for Large Eddy Simulation with Dynamic Estimation," *Journal of Computational Physics*, 186(2), 610-629.

Bull, MK (1996). "Wall-pressure Fluctuations Beneath Turbulent Boundary Layers: Some Reflections on Forty Years of Research," *Journal of Sound and Vibration*, 190(3), 299-315.

Fan, G, Zhao, W, and Wan, D (2025). "Near-wall Turbulent Fluctuations and Coherent Structures in Wall-modeled Large-eddy Simulation," *Physics of Fluids*, 37(9), 095108.

Guo, L, Li, D, Zhang, X, and He, G-W (2012). "LES Prediction of Space-time Correlations in Turbulent Shear Flows," *Acta Mech Sin*, 28(4), 993-998.

He, G, Jin, G, and Yang, Y (2017). "Space-Time Correlations and Dynamic Coupling in Turbulent Flows," *Annu Rev Fluid Mech*, 49(1), 51-70.

Jansson, N, Karp, M, Podobas, A, Markidis, S, and Schlatter, P (2024). "Neko: A Modern, Portable, and Scalable Framework for High-fidelity Computational Fluid Dynamics," *Computers & Fluids*, 275, 106243.

Karniadakis, GE (1989). "Spectral Element Simulations of Laminar and Turbulent Flows in Complex Geometries," *Applied Numerical Mathematics*, 6(1-2), 85-105.

Karp, M, Jansson, N, Podobas, A, Schlatter, P, and Markidis, S (2022a). "Reducing Communication in the Conjugate Gradient Method: A Case Study on High-order Finite Elements," *Proceedings of the Platform for Advanced Scientific Computing Conference*, Basel Switzerland, ACM, 1-11.

Karp, M, Podobas, A, Kenter, T, Jansson, N, Plessl, C, Schlatter, P, and Markidis, S (2022b). "A High-Fidelity Flow Solver for Unstructured Meshes on Field-Programmable Gate Arrays: Design, Evaluation, and Future Challenges," *International Conference on High Performance Computing in Asia-Pacific Region*, Virtual Event Japan, ACM, 125-136.

Patera, AT (1984). "A Spectral Element Method for Fluid Dynamics: Laminar Flow in a Channel Expansion," *Journal of Computational Physics*, 54(3), 468-488.

Shubham, S, Pargal, S, Moreau, S, Sandberg, RD, Yuan, J, Kushari, A, and Sanjose, M (2023). "Data-driven Empirical Wall pressure Spectrum Models for Fan Noise Prediction," *AIAA AVIATION 2023 Forum*, San Diego, CA and Online, American Institute of Aeronautics and Astronautics.

Wu, T, and He, G (2021). "Space-time Energy Spectra in Turbulent Shear Flows," *Phys Rev Fluids*, 6(10), 100504.

Yang, B, and Yang, Z (2022). "On the Wavenumber–frequency Spectrum of the Wall Pressure Fluctuations in Turbulent Channel Flow," *J Fluid Mech*, 937, A39.